JAMES | Journal of Advances in Modeling Earth Systems

RESEARCH ARTICLE
10.1029/2020MS002304

Nonlinear Increase of Vegetation Carbon Storage in Aging Forests and Its Implications for Earth System Models

Chen Zhu[1,2] and **Jianyang Xia**[1,2]

[1]Zhejiang Tiantong Forest Ecosystem National Observation and Research Station, Shanghai Key Lab for Urban Ecological Processes and Eco-Restoration, School of Ecological and Environmental Sciences, East China Normal University, Shanghai, China, [2]Research Center for Global Change and Ecological Forecasting, East China Normal University, Shanghai, China

Key Points:
- Observations constrain an exponential relationship in C_{veg} and f_w
- The exponential relationship in C_{veg} and f_w could be one useful benchmark for ESMs
- ESMs show divergent relationships between C_{veg} and forest age

Correspondence to:
J. Xia,
jyxia@des.ecnu.edu.cn

Citation:
Zhu, C., & Xia, J. (2020). Nonlinear increase of vegetation carbon storage in aging forests and its implications for Earth system models. *Journal of Advances in Modeling Earth Systems*, *12*, e2020MS002304. https://doi.org/10.1029/2020MS002304

Received 19 AUG 2020
Accepted 8 NOV 2020
Accepted article online 12 NOV 2020

Author Contributions:
Conceptualization: Jianyang Xia
Formal analysis: Chen Zhu, Jianyang Xia
Writing – review & editing: Chen Zhu, Jianyang Xia

Abstract Vegetation carbon stock (C_{veg}) in global forests, which is important for C cycle-climate feedbacks, commonly increases with forest age. Due to the allometric growth of plants, the nonlinear increase in C_{veg} with woody fraction (f_w) is expected across space. However, it remains unclear whether such a nonlinear relationship between C_{veg} and f_w can be constrained by observations and further used to benchmark Earth system models (ESMs). Here, based on the *in situ* measurements at 1,145 forest sites, we found that the nonlinear relationship between C_{veg} and f_w followed an exponential equation (i.e., $C_{veg} = be^{a \cdot f_w}$). Then, we showed that such an exponential dependence of C_{veg} on f_w also exists in ESMs of CMIP5 and CMIP6 (all $P < 0.01$), even though age-dependent processes have not been incorporated in most models. However, the exponential C_{veg}-f_w relationship varied greatly among the models, and the coefficient b was systematically lower in the ESMs (0.08 ± 0.11; mean $\pm$ SD) than the observations (0.28). Based on a compiled forest age data set, we further found that the observed nonlinear increase of C_{veg} with forest age across the Northern Hemisphere (>30°N) was not captured by ESMs. These findings reveal a high disagreement on the spatially nonlinear relationship between vegetation carbon stock and woody fraction in current ESMs. The exponential relationship based on observations provides one useful benchmark for ESMs when they implement the age-dependent processes in the future.

Plain Language Summary Forest age plays an important role in vegetation carbon stock (C_{veg}) predictions. This study detects a nonlinear increase of C_{veg} with woody fraction (f_w) in aging forests across 1,145 *in situ* observations. The nonlinear C_{veg}-f_w relationship was then used to benchmark the age impacts on C_{veg} predictions in Earth system models (ESMs). Combined with a global forest age data set, we show that current ESMs divergently represent the relationship between C_{veg} and forest age. Our study suggests that the C_{veg}-f_w relationship could be one useful benchmark for evaluating ESMs.

1. Introduction

The dynamics of vegetation carbon storage (C_{veg}) in northern temperate forests vary threefold among current Earth system models (ESMs) (Jiang et al., 2015; Xia et al., 2017). One potential reason for such uncertainty is that most ESMs typically averaged across all age classes and have poorly represented the age-dependent biogeochemical and ecological processes (Anderson-Teixeira et al., 2013). The important role of forest age in simulating vegetation carbon (C) storage has been validated by both big-leaf and tile-based models which have incorporated the age-related processes (Bayer et al., 2017; Shevliakova et al., 2009; Yue et al., 2018; Zaehle et al., 2006). For example, Zaehle et al. (2006) have incorporated the plant size-dependent C allocation in a big-leaf model (i.e., the Lund-Potsdam-Jena model), which then can better reproduce the observed present-day forest age structure and C_{veg} on the regional scale. The subgrid forest age structures have been implemented into some tile-based models, such as ORCHIDEE-MICT (Yue et al., 2018), LM3 (Shevliakova et al., 2009), JSBACH (Reick et al., 2013), and ISAM (Yang et al., 2010), allowing for the regional and global simulations of forest dynamics under land use changes. Recently, observations based on eddy flux towers have also shown that net CO_2 uptake of forest ecosystems is more controlled by forest age than climate (Besnard et al., 2018; Gao et al., 2016). As a result, the important role of forest age in determining vegetation C accumulation has been increasingly emphasized by both observational (Gough et al., 2016) and modeling

(Williams et al., 2012) studies. However, it remains unexamined that whether and how the simulation uncertainty or biases of C_{veg} in current ESMs are contributed from the inconsideration of forest age.

The ignorance of forest age impacts may lead to the biased modeling of C_{veg} in contrasting directions. On the one hand, numerous studies have reported that leaf area peaks at the early stage of forest development and followed by a reduction of photosynthesis in mature and old forests (Goulden et al., 2011; Gower et al., 1996; Law et al., 2003). Thus, one can expect an overestimation of C_{veg} in mature or old forests by models because of the lack of the age-related reduction in photosynthesis. Models can also underestimate the C_{veg} in young forests if the photosynthesis rates of mature or old forests are adopted. On the other hand, the allocation of net primary production to wood could increase with the forest age (Davidson et al., 2002; Peichl & Arain, 2006). Due to the longer C residence time in wood than other plant tissues (Bloom et al., 2016), ESMs could underestimate C_{veg} in mature and old forests if they incorrectly represent the age-related increase in woody C allocation. Current ESMs have simulated the dynamics of C allocation simply based on different indicators, such as NPP (e.g., NorESM1; Oleson et al., 2010) and tree height (e.g., GFDL; Shevliakova et al., 2009) or empirically by some allocation schemes, such as allometric scaling relationships (e.g., HadGEM2-CC; Clark et al., 2011) and resource availability (e.g., CanESM; Arora & Boer, 2005; IPSL; Krinner et al., 2005; MIROC; Sato et al., 2007). However, most of these allocation schemes have not explicitly represented the age impacts on C allocation. Thus, developing effective benchmarks for simulating the age impact on vegetation carbon stocks is urgently needed.

In recent years, the rapid development of new technology in Earth system science has promoted the benchmarking analyses on modeled C processes using observations (Collier et al., 2018; Luo et al., 2012; Reichstein et al., 2019). Some previous benchmarking analyses have shown that the ensemble mean of multiple ESMs can well capture the dynamics of gross primary production in global data products (Anav et al., 2013; Xia et al., 2020; Yan et al., 2014). However, benchmarking the performance of C_{veg} prediction in aging forests is still difficult because the C allocation scheme varies among models and different allocation schemes would cause large variability of predicted C_{veg} (Friedlingstein et al., 1999; Ise et al., 2010; Malhi et al., 2011). In mature and old forests, if the ESMs correctly simulate ecosystem productivity without considering the age impacts, one can hypothesize an underestimation of C_{veg} in these models. Because ESMs commonly lack the age-related increase in woody C allocation, we further hypothesize that current ESMs have led to a lower woody fraction (f_w) associated with the underestimated C_{veg} in mature and old forests. Thus, the relationship between C_{veg} and f_w could be a useful benchmark for evaluating the simulations of age impact on forest C_{veg} in the ESMs.

Here we explored the age-dependent increase of C_{veg} and f_w using *in situ* observations at 1,145 forest sites in northern temperature forests. Due to the allometric growth of trees (Niklas, 1995, 2004), the relationship between C_{veg} and f_w must be nonlinear (Poorter et al., 2015; Sheil et al., 2017; Sillett et al., 2010; Stephenson et al., 2014). Thus, we first explored whether the relationship between C_{veg} and f_w can be constrained by the observations. Then, we examined whether such a nonlinear relationship between C_{veg} and f_w also exits in current ESMs involved in the phases 5 and 6 of the Coupled Model Intercomparison Project (CMIP5 and CMIP6). Combined with a new global forest age database (Poorter et al., 2015), we further evaluated the age-related changes in C_{veg} in current ESMs against the observations. This study aims to (1) verify the relationship between C_{veg} and f_w in aging forests based on observations, (2) examine whether current two generations of ESMs capture the observed C_{veg}-f_w relationship, and (3) evaluate the effects of forest age on ESMs' performance in vegetation carbon predictions.

2. Methods

2.1. Data Sets

The allocations of the biomass of main tree compartments (leaves, stems, and roots) and total biomass data in this study were compiled from different data sources (Luo et al., 2014; Michaletz et al., 2014; Schepaschenko et al., 2017). We restricted our data selection to only those reported the forest age and biomass in the main tree compartments (leaves, stems, and roots). A complete list of data source references is provided in the Source Data file. Data were compiled for woody plants with latitude, longitude, and stand age as well as dry biomass of leaf, wood, root, and vegetation. Note that the stand age used in this study refers

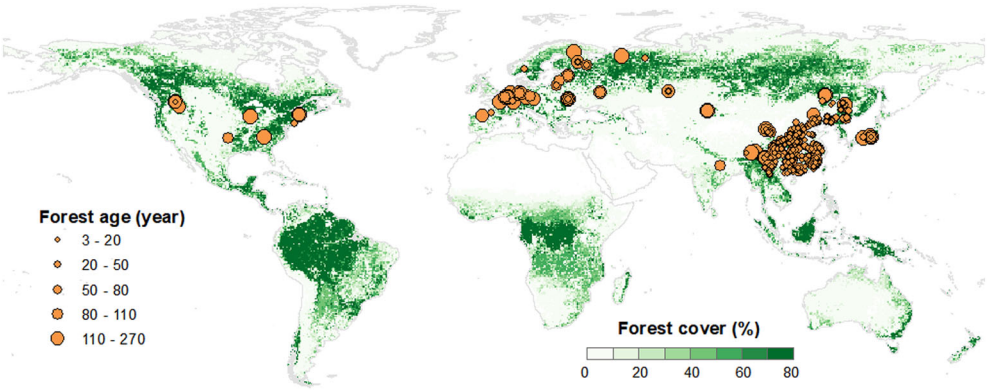

Figure 1. Locations of sample plots with observations of vegetation C and biomass in leaves, wood, and roots.

to the mean age of trees within the stand. The field data of China's forest biomass were collected from the Luo data set (Luo et al., 2014). That data set provides a wide range of survey data including 1,607 entries for 348 forest sites. We selected the records which reported the biomass of leaves, stems, roots, and vegetation. The Shvidenko data set (Schepaschenko et al., 2017) includes 10,351 records of sample plots for the periods of 1960–2014 in Eurasia. That data set reported the biomass of living trees as the stem, bark, branches, foliage, and roots, so the woody biomass was calculated by summing the stem, bark, and branches biomass. In the Shvidenko data set, we selected sites published after 1985 in each country that excluded China. The Michaletz data set was compiled from multiple data sources covering 1,247 stands and data records in boreal and temperate forests that are involved in our analyses (excluding China). Vegetation carbon storage was calculated as the total dry mass of stem, bark, branch, root and foliage components in the above three data sets. It should be noted that both natural and planted forests are included in these data sources. Because some data were measured from continuous forest inventory, there would be multiple records of different years in one region, and we treated these data as different stands. Finally, we got a total of 1,145 stands of northern temperate forests across Asia, Europe, and North America (Figure 1).

The forest age data were obtained from the global forest age data set (GFAD) (Poorter et al., 2015) with a resolution of 0.5° × 0.5° represents the 2000–2010 era. The GFAD data set was derived from the country-level forest inventory in most temperate and boreal regions and climate-specific stand age-biomass curves in the tropical areas. The original data were unified to 15 age classes defined in 10-yr intervals of forest type fractions: needleleaf evergreen, needleleaf deciduous, broadleaf evergreen, and broadleaf deciduous. The information on the fraction of forest within an age class in each grid cell is also provided by the GFAD data set. In each land grid cell, we first calculated the sum of the four forest type fractions. At each age class, we take the median of the age range and multiply the forest type fractions of each grid. We finally obtained the map of global forest age and extracted the ages of grid cells with the forest cover >50% across the Northern Hemisphere (>30°N).

The simulated biomass and vegetation carbon data from CMIP5 and CMIP6 ESMs were used to compared with *in situ* observations (Tables 1 and 2). In each modeling center, we only selected one model because the outputs from the same model center are very similar. Finally, eight ESMs from CMIP5 and seven ESMs from CMIP6 were used in this study. In ESMs, the total biomass and the biomass in leaves, stems, and roots are represented by cVeg, cLeaf, cWood, and cRoot. The monthly model outputs at the end of each year were extracted from historical runs during 2000–2005, which were then aggregated up to 0.5° × 0.5° resolution using the nearest neighbor interpolation. The ESMs data were restricted to the grid cells with the forest cover >50% across the Northern Hemisphere (>30°N).

2.2. Grouping of Forest Age Data

The forest age data were obtained from plot-level observations and grid-scale GFAD data set. The observation-based forest age data were binned into increments of 10 yr in the range of 0–130 yr in Figure 2a, then the observation-based C_{veg} were averaged in each forest age bin. The forest age data extracted from GFAD were binned into increments of 10 yr in the range of 0–130 yr in Figure 4. The values of forest age

Table 1
Information of CMIP5 ESMs Used in This Study

Model name	Modeling group	Land model	Allocation scheme	LUC	Original resolution	References
CanESM2	Canadian Center for Climate Modeling and Analysis	CTEM CLASS	Resource limitation	Yes	2.81° × 2.81°	Arora & Boer (2010)
IPSL-CM5A-LR	Institut Pierre-Simon Laplace	ORCHIDEE	Resource limitation	Yes	1.88° × 3.75°	Dufresne et al. (2013)
MRI-ESM 1	Meteorological Research Institute	HAL	Allometric relationship	No	1.13° × 1.13°	Yukimoto (2011)
Nor-ESM 1-M	Norwegian Climate Center	CLM 4.0	Dynamic functions of NPP	Yes	1.88° × 2.50°	Tjiputra et al. (2013)
CCSM4	National Center for Atmospheric Research	CLM 4.0	Dynamic functions of NPP	Yes	1.25° × 0.94°	Gent et al. (2011)
GFDL-ESM 2G	NOAA Geophysical Fluid Dynamics Laboratory	LM 3.0	Tree height	Yes	1.99° × 2.48°	Dunne et al. (2013)
HadGEM2-CC	Met Office Hadley Center (additional HadGEM2-ES realizations contributed by Instituto Nacional de Pesquisas Espaciais)	JULES TRIFFID	Allometric relationship based on leaf area index	Yes	1.24° × 1.88°	Collins et al. (2011)
MIROC-ESM	Japan Agency for Marine-Earth Science and Technology, Atmosphere and Ocean Research Institute (The Institute for Environmental Studies University of Tokyo), and National	MATSIRO SEIB-DGVM	Environmental conditions at tree level	Yes	2.81° × 2.81°	Watanabe et al. (2011)

Note. LUC = land use change.

larger than 130 yr in observations and GFAD were binned into one group because the number of samples is relatively small. The bin size ensured that each bin size contains more than five samples. In each age group, the C_{veg} of each of the 15 models in two CMIPs was also averaged. Linear or nonlinear regression was applied to detect the dependence of C_{veg} on binned forest age in observations and ESMs, respectively.

To reduce the uncertainty from scale mismatch between the plot-level observations and gridded products, the *in situ* measurements were weighted based on the fraction of the forest provided by the GFAD dataset to match grid cells. So the *in situ* measurements of biomass data were averaged to 15 age classes defined in 10-yr intervals, from 1–10 up to a class greater than 150 years old. Then the weighted biomass of each grid cell was calculated based on the averaged biomass data of each age class and the proportion of forest at each grid cell. The relationship between the weighted C_{veg} and the gridded forest age data was plotted in Figure 2a.

Table 2
Information of CMIP6 ESMs Used in This Study

Model name	Modeling group	Land model	Allocation scheme	LUC	Original resolution	References
CanESM5	Canadian Center for Climate Modeling and Analysis	CTEM CLASS	Resource limitation	Yes	2.81° × 2.81°	Swart et al. (2019)
IPSL-CM6A-LR	Institut Pierre-Simon Laplace	ORCHIDEE	Resource limitation	Yes	1.88° × 3.75°	Boucher et al. (2020)
MRI-ESM 2-0	Meteorological Research Institute	HAL	Allometric relationship	Yes	1.13° × 1.13°	Yukimoto et al. (2019)
NorESM2-LM	Norwegian Climate Center	CLM5.0	Fixed coefficient	Yes	1.88° × 2.50°	Seland et al. (2020)
CESM2	National Center for Atmospheric Research	CLM 5.0	Fixed coefficient	Yes	0.94° × 1.25°	Lawrence et al. (2019)
ACCESS-ESM 1-5	Commonwealth Scientific and Industrial Research Organization	CABLE2.4	Fixed coefficient	No	1.875° × 1.25°	Law et al. (2017)
CNRM-ESM 2	National Center for Meteorological Research, Météo-France and CNRS laboratory	ISBA-CTRIP	Related with plant N decline model	Yes	1.4° × 1.4°	Séférian et al. (2019)

Note. LUC = land use change.

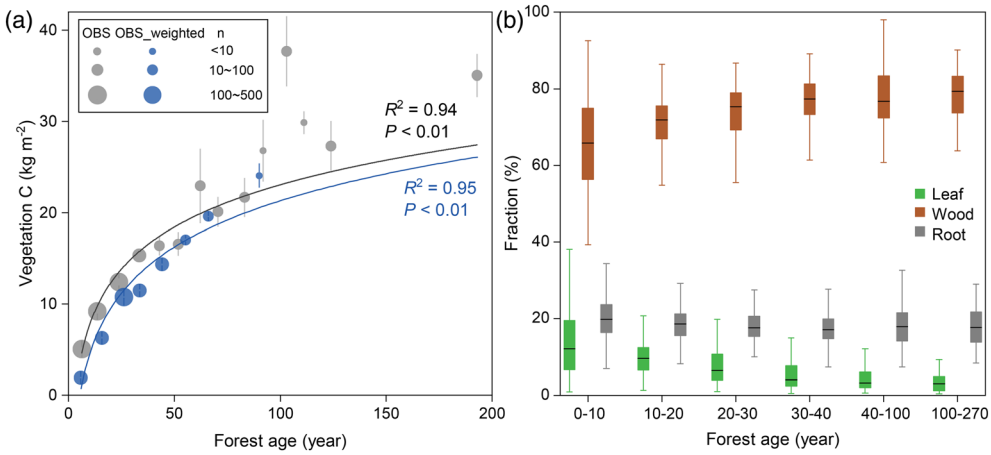

Figure 2. Age-dependent (a) vegetation carbon stocks and (b) biomass fractions of leaves, wood, and roots in *in situ* measurements. The dark gray curve in (a) represents the fitting of observation-derived data to a logarithmic regression model as $C_{veg} = 6.67 \ln(\text{Age}) - 7.67$ ($R^2 = 0.94$, $P < 0.01$). The blue curve represents in (a) the fitting of weighted observational data to a logarithmic regression model as $C_{veg} = 7.31 \ln(\text{Age}) - 12.37$ ($R^2 = 0.95$, $P < 0.01$). The size of each point represents the number of sites in each bin size. The vertical gray bars indicate the standard errors. Boxes in (b) indicate the 25% and 75% quartiles, whiskers indicate the extent of the data, and lines indicate the median.

3. Results

3.1. Age-Dependent Nonlinear Increase of C_{veg} and f_w in Observations

By plotting the observation-based vegetation carbon stocks with forest age, we found that C_{veg} increased nonlinearly with forest age across all 1,145 forest sites ($R^2 = 0.94$, $P < 0.01$; Figure 2a). The biomass allocated to wood increased in young forests and then gradually saturated in old forests (Figure 2b). The partitioning of leaf biomass rapidly reduced in the young forest and then slowly reduced in old forests (Figure 2b). The biomass allocated to roots declined at the early stage and but raised when the forests were older than ~100 years old (Figure 2b). Across the 1,145 forest sites, trees kept accumulating carbon in wood as they age, and the C_{veg} exponentially increased with f_w ($R^2 = 0.26$, $P < 0.01$; Figure 3).

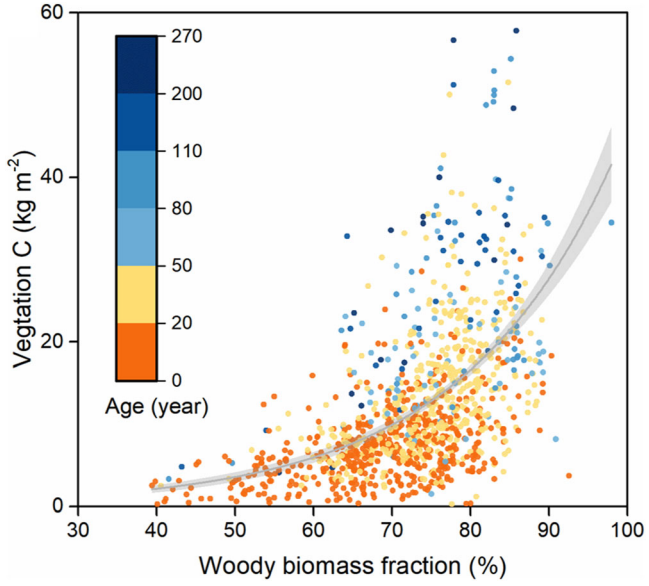

Figure 3. The dependence of vegetation carbon stocks on woody biomass fractions in *in situ* measurements. The curve represents the fitting of data to an exponential model as $C_{veg} = be^{a \cdot f_w}$ ($a = 0.05$, $b = 0.28$; $R^2 = 0.26$, $P < 0.01$).

3.2. The Nonlinear Relationship Between C_{veg} and f_w in Earth System Models

Spatially, areas with high f_w fractions corresponded to large C_{veg} (Figure 4). The evolution of models from CMIP5 to CMIP6 has resulted in larger carbon stock and higher f_w in northern Canada, Eastern United States, Northeast Europe, and Western Siberia (Figures 4a, 4c, 4e, and 4g). However, the increase of C_{veg} and f_w did not add uncertainty in these regions except in the Eastern United States (Figures 4b, 4d, 4f, and 4h).

Although all eight ESMs in CMIP5 and seven ESMs in CMIP6 captured the exponential dependence of C_{veg} on f_w (all $P < 0.01$; Figures 5a and 5b and Table 3), the parameters in the exponential relationship (i.e., $C_{veg} = be^{a \cdot f_w}$) between woody biomass fraction and vegetation carbon varied greatly among models. The coefficient a in the exponential function estimated for observations was smaller than that in all ESMs except IPSL-CM5A-LR, ACCESS-ESM 1-5, and CNRM-ESM 2 (Table 3). The coefficients b estimated for all ESMs ranged from 0.42×10^{-6} to 0.32, which were smaller than that from the observations except ACCESS-ESM 1-5 (Table 3). The five models that participated in both CMIPs also show divergent C_{veg}-f_w relationship in CMIP5 and CMIP6.

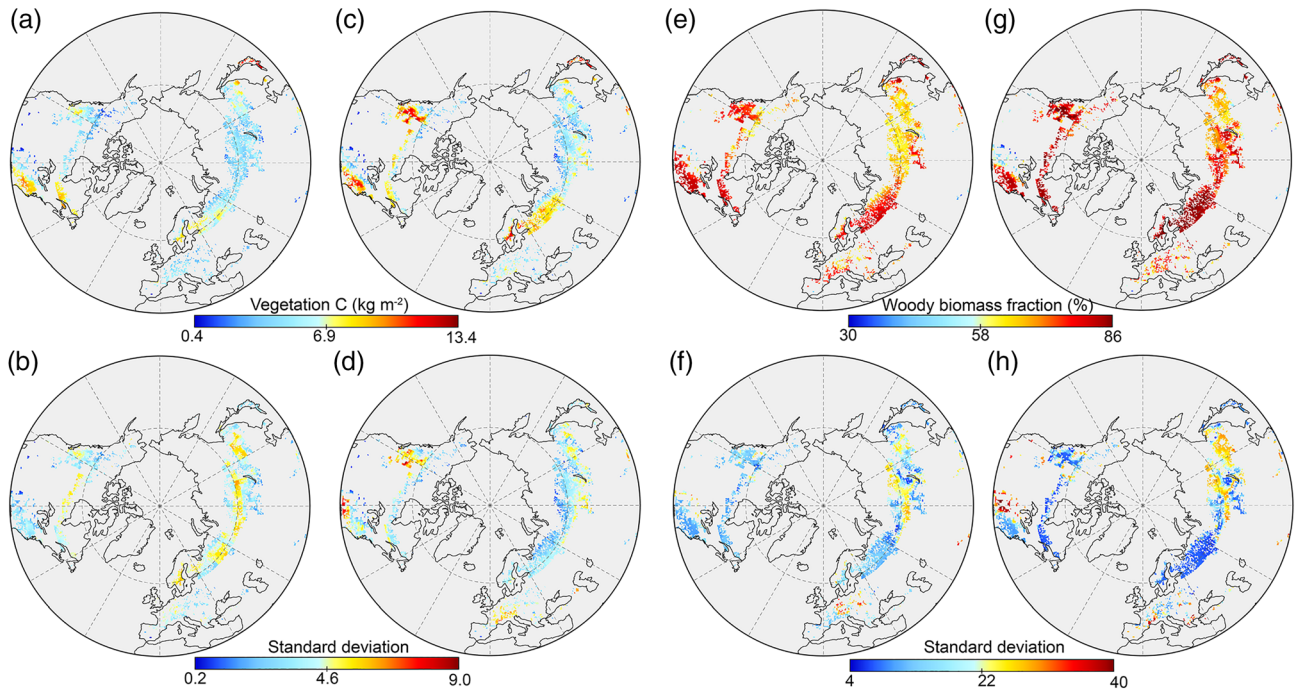

Figure 4. Spatial distributions of vegetation C, woody biomass fraction, and corresponding standard deviation. The multimodel average of vegetation C and woody biomass fraction during 2000–2005 for (a, e) CMIP5 and (c, g) CMIP6 ESMs. The standard deviation across models of vegetation C and woody biomass fraction for (b, f) CMIP5 and (d, h) CMIP6 ESMs.

3.3. Relationships of Modeled C_{veg} to Age

Although the forest age has not been explicitly considered in ESMs, we examined whether they captured the observed age-dependent nonlinear increase of C_{veg} by plotting the modeled C_{veg} against the GFAD forest age. We found that the CMIP5 and CMIP6 models captured few the nonlinear increase of C_{veg} with forest age in grid cells across the forest region of the Northern Hemisphere (Figure 6). In many cases, the modeled C_{veg} in CMIP5 and CMIP6 tended to be saturated with forest age (Figures 6a and 6b). Some models showed an increase of C_{veg} at the early stage and then significantly decreased with forest age (Figures 6a and 6b). On the contrary, MIROC-ESM exhibited a linear increase of C_{veg} with forest age (Figure 6a).

3.4. Comparison of Biomass Allocation Among ESMs

We presented the allocation fractions of biomass in leaves, wood, and roots for each model over 2000–2005 (Figure 7). The results showed large model-to-model differences in wood biomass allocation (from 0.62 in IPSL-CM6A-LR to 0.88 in CNRM-ESM 2), leaf biomass allocation (from 0.008 in CNRM-ESM 2 to 0.13 in NorESM1-M), and root biomass allocation (from 0.06 in IPSL-CM5A-LR to 0.37 in MRI-ESM 1). The four (IPSL-CM5A-LR, MRI-ESM 1, NorESM1-M, and CCSM4) out of five models that participated in both CMIPs show a large disagreement on the woody biomass allocation between the two CMIPs. The CanESM2 in CMIP5 and CanESM5 in CMIP6 showed very similar biomass allocation in leaves, wood, and roots.

4. Discussions

4.1. The Emergent C_{veg}-f_w Relationship in Observations and ESMs

This study detects an age-dependent increase in both of f_w and C_{veg} (Figure 2) and then constrains an exponential relationship between f_w and C_{veg} based on the *in situ* observations (Figure 3). This relationship is different from a previous study which has shown an *S*-type nonlinear correlation between f_w and C_{veg} based on observations of tree seedlings (Poorter et al., 2015). The exponential relationship found in this study could be partially explained by the changes in biomass allocation at different growth stages (Figure 2b). At the early stage of tree growth, trees increase in size and height to maintain structural support and other physical

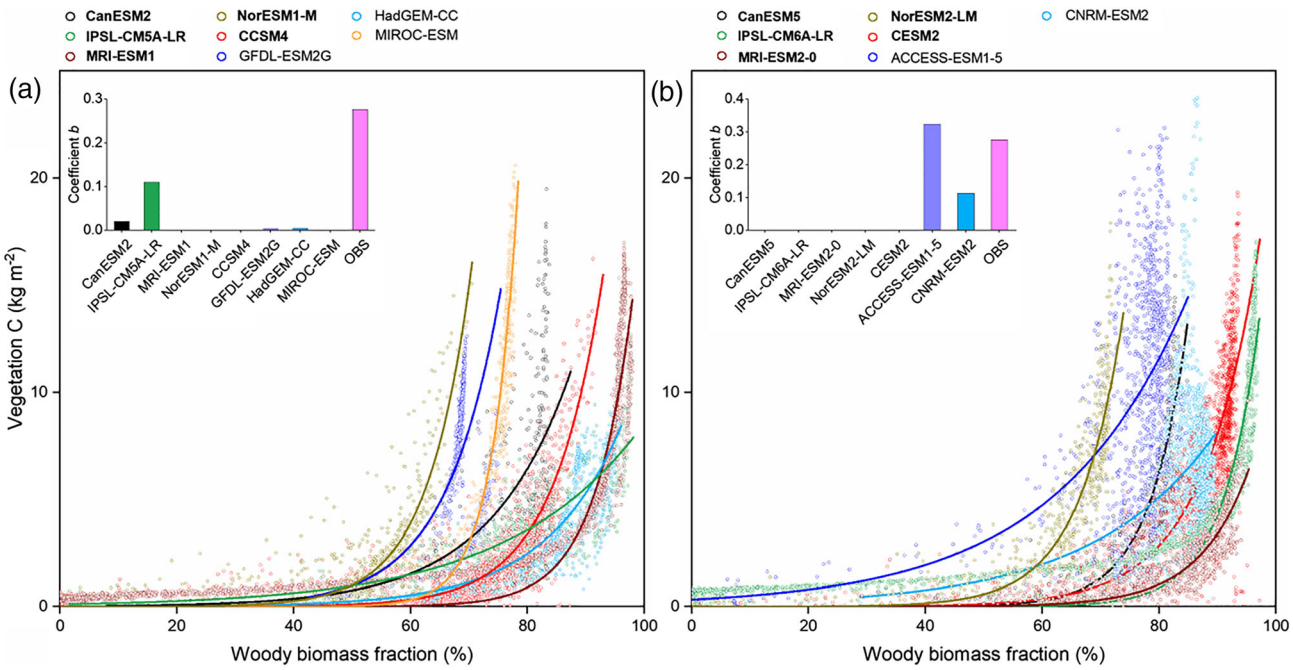

Figure 5. Nonlinear dependence of vegetation C on the woody fraction in (a) CMIP5 and (b) CMIP6 ESMs. The inset panels show the ranges of coefficients *b* in each model. The ESM name in bold indicates the model participating in two phases of CMIP but in different versions.

requirements (Niklas, 2004; West et al., 1999). After establishment, wood biomass allocation would continue to increase to support the diameter growth and the more complex crown structures (Phillips et al., 2008; Sillett et al., 2010; Van Pelt & Sillett, 2008). Thus, the exponential increase of C_{veg} with f_w validated in this study is an emergent property driven by multiple mechanisms of C accumulation during forest development.

Even without age-related processes, the ESMs can produce the exponential relationship between f_w and C_{veg}. However, such an exponential relationship is divergent among the 15 ESMs (Figure 5). It means that the coefficients of the exponential equation based on observations can be useful in diagnosing the model performance on forest C_{veg}. For example, the coefficient *b* is lower in all ESMs except ACCESS-ESM-1-5 than the observations (Figure 5 inset), indicating that the models systematically underestimated the C_{veg} in low f_w. On the contrary, the coefficient *a* in most ESMs is larger than the observations (Table 3). A higher coefficient *a* means the rapid increase of C_{veg} with f_w, which indicates a more converging f_w at a specific range of C_{veg}. These findings suggest that the exponential relationship between f_w and C_{veg} across space provides an important benchmark for evaluating ESMs in forest carbon cycle.

Table 3
Parameters in the Relationship Between Woody Biomass Fraction and Vegetation Carbon for 14 ESMs and In Situ Observations

	a	*b*	*p*	R^2
OBS	0.05119	0.27635	<0.01	0.26
CMIP5				
CanESM2	0.0717	0.0208	<0.01	0.23
IPSL-CM5A-LR	0.04353	0.11024	<0.01	0.68
MRI-ESM 1	0.15446	0.39×10^{-5}	<0.01	0.89
NorESM1-M	0.13488	0.00119	<0.01	0.75
CCSM4	0.11733	0.28×10^{-3}	<0.01	0.76
GFDL-ESM 2G	0.1068	0.0047	<0.01	0.36
HadGEM-CC	0.07663	0.00536	<0.01	0.83
MIROC-ESM	0.22523	0.42×10^{-6}	<0.01	0.85
CMIP6				
CanESM5	0.15469	0.26×10^{-4}	<0.01	0.72
IPSL-CM6A-LR	0.15996	0.24×10^{-5}	<0.01	0.89
MRI-ESM 2-0	0.11876	0.78×10^{-4}	<0.01	0.72
NorESM2-LM	0.13272	0.76×10^{-3}	<0.01	0.65
CESM2	0.10432	0.68×10^{-3}	<0.01	0.66
ACCESS-ESM 1-5	0.0447	0.3243	<0.01	0.4
CNRM-ESM 2	0.0476	0.1133	<0.01	0.1

4.2. The Evaluation on the Simulations of Age Impacts on C_{veg} in ESMs

Based on a compiled forest age data set, either linear or nonlinear relationship between C_{veg} and forest age is detected in the ESMs (Figure 6). The linear increase of C_{veg} with age is simulated by MIROC, which adopts an individual-based approach to simulate trees establish, competition, and mortality, and enables the large trees to persist for a long time under favorable sunlight conditions (Sato et al., 2007). The nonlinear relationship between C_{veg} and forest age varies among different models (Figures 6a and 6b). The majority of ESMs simulate a saturation of C_{veg} with forest age, while some ESMs simulate a rapid decline of C_{veg} after the early stage of forest development. The observed nonlinear increasing trend of C_{veg} with forest age in this study (Figure 2a) is in line with the new idea in

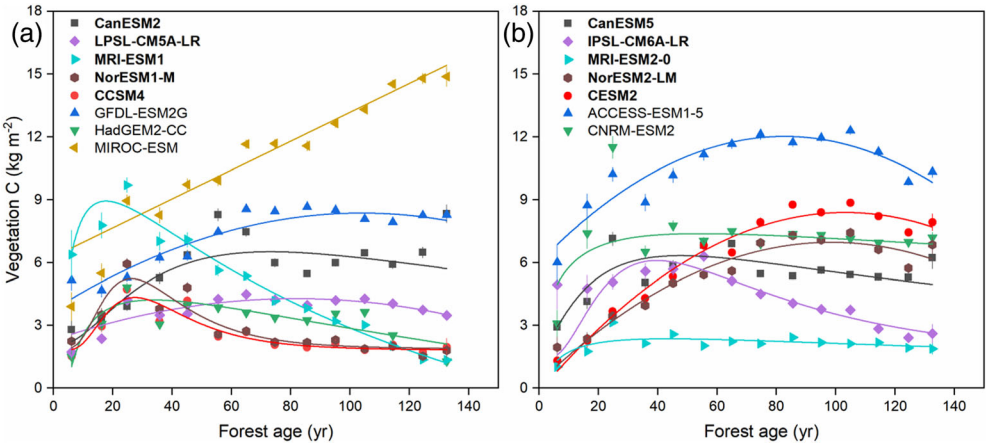

Figure 6. The dependence of vegetation carbon stocks on forest age in (a) CMIP5 and (b) CMIP6 ESMs (all $P < 0.01$). The ESM name in bold indicates the model participating in two phases of CMIP but in different versions.

ecology that aging forests keep accumulating carbon (Curtis & Gough, 2018; Stephenson et al., 2014). In addition, the nonlinear relationship between C_{veg} and forest age in some models substantially changes from CMIP5 to CMIP6 (Figures 6a and 6b). For example, the C_{veg} increases at the early stage then rapidly decreases with forest age in MRI-ESM 1 but keeps a relatively low value and saturated with forest age in MRI-ESM 2-0, which could be due to the incorporation of land use changes in MRI-ESM 2-0.

The saturated or decreasing trend in C_{veg} with forest age in ESMs could result from two apparent reasons. First, the vegetation C residence time in most CMIP5 models is shorter than 15 yr at the global scale (Jiang et al., 2015) and is rarely longer than 50 yr in forest regions (Wu et al., 2018). The short vegetation C residence time mainly results from the biased parameterizations of C age in different plant tissues (Cui et al., 2019). Second, the biomass allocation to wood is low in some models (Figure 7), which limits the C storage capacity of vegetation in the models.

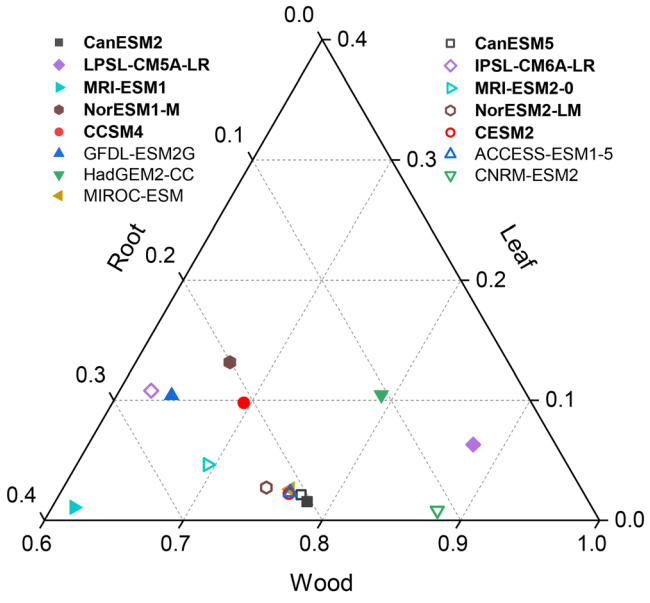

Figure 7. The biomass allocation to leaves, wood, and roots in CMIP5 and CMIP6 ESMs. The ESM name in bold indicates the model participating in two phases of CMIP but in different versions.

4.3. The Important Role of Biomass Allocation in the C_{veg}-f_w Relationship

Many allocation schemes have been developed to model the dynamics of C allocation in plants in the past two decades (Franklin et al., 2012). The various allocation schemes have produced widespread biomass allocation fractions among leaves, wood, and roots in current ESMs (Figure 7). In those C allocation schemes, the models use an allometric approach (MRI-ESM 1 and MRI-ESM 2-0; Sitch et al., 2003) and dynamic function of annual NPP (CCSM4 and NorESM1-M; Oleson et al., 2010) that usually simulate less biomass allocation to wood (Figure 7). The modeled low f_w would correspond to a significant declining trend of C_{veg} in the aging forest in CCSM4, MRI-ESM 1, and NorESM1-M (Figure 6a). In contrast, the models based on resource limitations approach (CanESM2 and CanESM5; Arora & Boer, 2005; IPSL-CM5A-LR and IPSL-CM6A-LR, Krinner et al., 2005), plant N decline model (CNRM-ESM 2; Gibelin et al., 2006), and leaf area index (HadGEM2-CC; Clark et al., 2011) can allocate more biomass to the woods (Figure 7). However, a saturation rather than an increase of C_{veg} in aging forest was captured by these models (Figure 6). Such a saturation pattern is consistent with the modeling results in a recent study, which found that the allocations ratios among leaves, woods, and roots only change in young forests (Xia et al., 2019). It also should be noted that some vegetation processes and environmental factors can influence the C allocation patterns. For example, the wood C fraction modeled by IPSL-CM5A-LR in CMIP5 was 0.88 but decreased to 0.62 by IPSL-CM6A-LR in CMIP6, the latter of which has taken consideration

of the annual evolution of the plant functional type maps (Boucher et al., 2020). The reduced f_w partially explains the different relationships between C_{veg} and forest age in IPSL-CM5A-LR and IPSL-CM6A-LR (Figures 6a and 6b). The environmental factors such as high temperature and drought stress would force a reduction of wood allocation (Zhu et al., 2020).

Although the majority of ESMs have not explicitly represented the age-dependent biomass allocation in their vegetation model, rapid developments have been achieved recently in the offline land-surface models. In vegetation demographic models, the subgrid forest age structure is inherently provided at individual or cohort levels. For example, the CLM (ED) (Fisher et al., 2015), the LPJ-GUESS (Smith, 2001), and the SEIB-DGVM (Sato et al., 2007) have represented the spatial variability of the individual age or individual trees with the same age. In big-leaf or tile-based models, there are two approaches to introduce the subgrid forest age. The first approach is to incorporate a vegetation demographic model, such as the CABLE-POP model (Haverd et al., 2018) by coupling a vegetation demographic model (i.e., POP) to a big-leaf model (i.e., CABLE). The other approach is to increase the number of tiles to represent age structures of different subgrids. For example, the LM3V model uses multiple tiles within each land grid cell to capture the age distribution of vegetation (Shevliakova et al., 2009). A recent version of the ORCHIDEE model (i.e., ORCHIDEE-MICT; Yue et al., 2018) has represented vegetation age structure based on multiple subgrid patches.

4.4. Uncertainty and Limitations

Several limitations of this study should be noticed. First, the observations are based on the plot inventories from different studies, so they have inevitable uncertainty from sampling selections, measurement errors, and allometric growth fitting (Cunia, 1965). Second, the distribution of the data used in this study concentrated on China (Figure 1), which may impact the C_{veg}-f_w relationship. The forest age for Chinese forests is relatively young (Zhang et al., 2017); thus, only a small proportion of the observations are from old forests (e.g., >140 yr; McDowell et al., 2020) (Figure 2a). Adding more observations from old forests could alter the parameters in the exponential relationship between C_{veg} and f_w as found in this study (i.e., $C_{veg} = be^{a \cdot f_w}$). Third, the historical land use change has been incorporated in most ESMs (Table 1) but natural disturbances are rarely considered. It should be expected to result in smaller forest biomass in ESMs outputs because of the underestimation of C uptake in regrowth forests without considering natural disturbances (Pugh et al., 2019). Ignoring the increased frequency and severity of nature disturbances (e.g., large wildfires and bark beetles) can also lead to an overestimation of vegetation carbon (Seidl et al., 2014). Lastly, it should be noted that the spatial scale mismatch adds uncertainty to the data-model comparison in this study. To reduce such uncertainty, we further weighted the observations to match grid cells. The pattern between the weighted C_{veg} and the gridded forest age data was the same as that of the observation-based (Figure 2a).

5. Conclusions

In summary, this study detects an age-dependent nonlinear increase in C_{veg} and f_w, and reveals an exponential C_{veg}-f_w relationship in observations. The C_{veg}-f_w relationship exists but varies greatly in ESMs which participated in CMIP5 and CMIP6. Further analyses provide some important recommendations to ESMs. First, current ESMs need to better capture the observed nonlinear increase of C_{veg} with forest age. Second, the efforts of improving vegetation C allocation in ESMs (De Kauwe et al., 2014; Negrón-Juárez et al., 2015; Song et al., 2017) should take forest age into consideration. Third, global data products of forest age and vegetation C allocation are helpful to constrain the C_{veg}-f_w relationship on the global scale. Overall, this study highlights the important role of forest age in estimating vegetation carbon storage and provides an observation-derived C_{veg}-f_w relationship to benchmark forest carbon stocks in Earth system models.

Conflict of Interest

The authors declare no competing financial interests.

Data Availability Statement

The model simulations analyzed in this study were obtained from the Earth System Grid Federation CMIP5 online portal hosted by the Program for Climate Model Diagnosis and Intercomparison at Lawrence

Livermore National Laboratory (https://pcmdi.llnl.gov/projects/esgf-llnl/). The data used for the preparation of the figures are publicly available (https://doi.pangaea.de/10.1594/PANGAEA.897395). Observational data analyzed in this work have been deposited in figshare (https://doi.org/10.6084/m9.figshare.13180649.v1).

Acknowledgments
We thank the two anonymous reviewers for their constructive comments and suggestions. This study was supported by the National Key R&D Program (2017YFA0604600) and the National Natural Science Foundation of China (31722009).

References

Anav, A., Friedlingstein, P., Kidston, M., Bopp, L., Ciais, P., Cox, P., et al. (2013). Evaluating the land and ocean components of the global carbon cycle in the CMIP5 Earth system models. *Journal of Climate*, *26*(18), 6801–6843. https://doi.org/10.1175/JCLI-D-12-00417.1

Anderson-Teixeira, K. J., Miller, A. D., Mohan, J. E., Hudiburg, T. W., Duval, B. D., & Delucia, E. H. (2013). Altered dynamics of forest recovery under a changing climate. *Global Change Biology*, *19*(7), 2001–2021. https://doi.org/10.1111/gcb.12194

Arora, V., & Boer, G. (2010). Uncertainties in the 20th century carbon budget associated with land use change. *Global Change Biology*, *16*(12), 3327–3348. https://doi.org/10.1111/j.1365-2486.2010.02202.x

Arora, V. K., & Boer, G. J. (2005). A parameterization of leaf phenology for the terrestrial ecosystem component of climate models. *Global Change Biology*, *11*(1), 39–59. https://doi.org/10.1111/j.1365-2486.2004.00890.x

Bayer, A. D., Lindeskog, M., Pugh, T. A. M., Anthoni, P. M., Fuchs, R., & Arneth, A. (2017). Uncertainties in the land-use flux resulting from land-use change reconstructions and gross land transitions. *Earth System Dynamics*, *8*(1), 91–111. https://doi.org/10.5194/esd-8-91-2017

Besnard, S., Carvalhais, N., Arain, M. A., Black, A., de Bruin, S., Buchmann, N., et al. (2018). Quantifying the effect of forest age in annual net forest carbon balance. *Environmental Research Letters*, *13*(12), 124018. https://doi.org/10.1088/1748-9326/aaeaeb

Bloom, A. A., Exbrayat, J. F., van der Velde, I. R., Feng, L., & Williams, M. (2016). The decadal state of the terrestrial carbon cycle: Global retrievals of terrestrial carbon allocation, pools, and residence times. *Proceedings of the National Academy of Sciences of the USA*, *113*(5), 1285–1290. https://doi.org/10.1073/pnas.1515160113

Boucher, O., Servonnat, J., Albright, A. L., Aumont, O., Balkanski, Y., Bastrikov, V., et al. (2020). Presentation and evaluation of the IPSL-CM6A-LR climate model. *Journal of Advances in Modeling Earth Systems*, *12*, e2019MS002010. https://doi.org/10.1029/2019MS002010

Clark, D. B., Mercado, L. M., Sitch, S., Jones, C. D., Gedney, N., Best, M. J., et al. (2011). The Joint UK Land Environment Simulator (JULES), model description—Part 2: Carbon fluxes and vegetation dynamics. *Geoscientific Model Development*, *4*(3), 701–722. https://doi.org/10.5194/gmd-4-701-2011

Collier, N., Hoffman, F. M., Lawrence, D. M., Keppel-Aleks, G., Koven, C. D., Riley, W. J., et al. (2018). The International Land Model Benchmarking (ILAMB) System: Design, theory, and implementation. *Journal of Advances in Modeling Earth Systems*, *10*, 2731–2754. https://doi.org/10.1029/2018MS001354

Collins, W. J., Bellouin, N., Doutriaux-Boucher, M., Gedney, N., Halloran, P., Hinton, T., et al. (2011). Development and evaluation of an Earth-system model – HadGEM2. *Geoscientific Model Development Discussions*, *4*(2), 997–1062. https://doi.org/10.5194/gmdd-4-997-2011

Cui, E., Huang, K., Arain, M. A., Fisher, J. B., Huntzinger, D. N., Ito, A., et al. (2019). Vegetation functional properties determine uncertainty of simulated ecosystem productivity: A traceability analysis in the East Asian monsoon region. *Global Biogeochemical Cycles*, *33*, 668–689. https://doi.org/10.1029/2018GB005909

Cunia, T. (1965). Some theory on reliability of volume estimates in a forest inventory sample. *Forest Science*, *11*(1), 115–128. https://doi.org/10.1093/forestscience/11.1.115

Curtis, P. S., & Gough, C. M. (2018). Forest aging, disturbance and the carbon cycle. *New Phytology*, *219*(4), 1188–1193. https://doi.org/10.1111/nph.15227

Davidson, E. A., Savage, K., Bolstad, P., Clark, D. A., Curtis, P. S., Ellsworth, D. S., et al. (2002). Belowground carbon allocation in forests estimated from litterfall and IRGA-based soil respiration measurements. *Agricultural and Forest Meteorology*, *113*(1–4), 39–51. https://doi.org/10.1016/s0168-1923(02)00101-6

De Kauwe, M. G., Medlyn, B. E., Zaehle, S., Walker, A. P., Dietze, M. C., Wang, Y. P., et al. (2014). Where does the carbon go? A model-data intercomparison of vegetation carbon allocation and turnover processes at two temperate forest free-air CO_2 enrichment sites. *New Phytology*, *203*(3), 883–899. https://doi.org/10.1111/nph.12847

Dufresne, J. L., Foujols, M. A., Denvil, S., Caubel, A., Marti, O., Aumont, O., et al. (2013). Climate change projections using the IPSL-CM5 Earth system model: From CMIP3 to CMIP5. *Climate Dynamics*, *40*(9–10), 2123–2165. https://doi.org/10.1007/s00382-012-1636-1

Dunne, J. P., John, J. G., Shevliakova, E., Stouffer, R. J., Krasting, J. P., Malyshev, S. L., et al. (2013). GFDL's ESM 2 global coupled climate-carbon Earth system models. Part II: Carbon system formulation and baseline simulation characteristics. *Journal of Climate*, *26*(7), 2247–2267. https://doi.org/10.1175/JCLI-D-12-00150.1

Fisher, R. A., Muszala, S., Verteinstein, M., Lawrence, P., Xu, C., McDowell, N. G., et al. (2015). Taking off the training wheels: The properties of a dynamic vegetation model without climate envelopes, CLM4.5(ED). *Geoscientific Model Development*, *8*(11), 3593–3619. https://doi.org/10.5194/gmd-8-3593-2015

Franklin, O., Johansson, J., Dewar, R. C., Dieckmann, U., McMurtrie, R. E., Brannstrom, A., & Dybzinski, R. (2012). Modeling carbon allocation in trees: A search for principles. *Tree Physiology*, *32*(6), 648–666. https://doi.org/10.1093/treephys/tpr138

Friedlingstein, P., Joel, G., Field, C. B., & Fung, I. Y. (1999). Toward an allocation scheme for global terrestrial carbon models. *Global Change Biology*, *5*(7), 755–770. https://doi.org/10.1046/j.1365-2486.1999.00269.x

Gao, S., Zhou, T., Zhao, X., Wu, D., Li, Z., Wu, H., et al. (2016). Age and climate contribution to observed forest carbon sinks in East Asia. *Environmental Research Letters*, *11*(3), 034021. https://doi.org/10.1088/1748-9326/11/3/034021

Gent, P. R., Danabasoglu, G., Donner, L. J., Holland, M. M., Hunke, E. C., Jayne, S. R., et al. (2011). The community climate system model version 4. *Journal of Climate*, *24*(19), 4973–4991. https://doi.org/10.1175/2011JCLI4083.1

Gibelin, A.-L., Calvet, J.-C., Roujean, J.-L., Jarlan, L., & Los, S. O. (2006). Ability of the land surface model ISBA-A-gs to simulate leaf area index at the global scale: Comparison with satellites products. *Journal of Geophysical Research*, *111*, D18102. https://doi.org/10.1029/2005JD006691

Gough, C. M., Curtis, P. S., Hardiman, B. S., Scheuermann, C. M., & Bond-Lamberty, B. (2016). Disturbance, complexity, and succession of net ecosystem production in North America's temperate deciduous forests. *Ecosphere*, *7*(6), e01642. https://doi.org/10.1002/ecs2.1375

Goulden, M. L., McMillan, A. M. S., Winston, G. C., Rocha, A. V., Manies, K. L., Harden, J. W., & Bond-Lamberty, B. P. (2011). Patterns of NPP, GPP, respiration, and NEP during boreal forest succession. *Global Change Biology*, *17*(2), 855–871. https://doi.org/10.1111/j.1365-2486.2010.02274.x

Gower, S. T., McMurtrie, R. E., & Murty, D. (1996). Aboveground net primary production decline with stand age: Potential causes. *Trends in Ecology & Evolution*, *11*(9), 378–382. https://doi.org/10.1016/0169-5347(96)10042-2

Haverd, V., Smith, B., Nieradzik, L., Briggs, P. R., Woodgate, W., Trudinger, C. M., et al. (2018). A new version of the CABLE land surface model (subversion revision r4601) incorporating land use and land cover change, woody vegetation demography, and a novel optimisation-based approach to plant coordination of photosynthesis. *Geoscientific Model Development*, *11*(7), 2995–3026. https://doi.org/10.5194/gmd-11-2995-2018

Ise, T., Litton, C. M., Giardina, C. P., & Ito, A. (2010). Comparison of modeling approaches for carbon partitioning: Impact on estimates of global net primary production and equilibrium biomass of woody vegetation from MODIS GPP. *Journal of Geophysical Research*, *115*, G04025. https://doi.org/10.1029/2010JG001326

Jiang, L., Yan, Y., Hararuk, O., Mikle, N., Xia, J., Shi, Z., et al. (2015). Scale-dependent performance of CMIP5 Earth system models in simulating terrestrial vegetation carbon*. *Journal of Climate*, *28*(13), 5217–5232. https://doi.org/10.1175/jcli-d-14-00270.1

Krinner, G., Viovy, N., de Noblet-Ducoudré, N., Ogée, J., Polcher, J., Friedlingstein, P., et al. (2005). A dynamic global vegetation model for studies of the coupled atmosphere-biosphere system. *Global Biogeochemical Cycles*, *19*, GB1015. https://doi.org/10.1029/2003GB002199

Law, B. E., Sun, O. J., Campbell, J., Van Tuyl, S., & Thornton, P. E. (2003). Changes in carbon storage and fluxes in a chronosequence of ponderosa pine. *Global Change Biology*, *9*(4), 510–524. https://doi.org/10.1046/j.1365-2486.2003.00624.x

Law, R. M., Ziehn, T., Matear, R. J., Lenton, A., Chamberlain, M. A., Stevens, L. E., et al. (2017). The carbon cycle in the Australian Community Climate and Earth System Simulator (ACCESS-ESM 1)—Part 1: Model description and pre-industrial simulation. *Geoscientific Model Development*, *10*(7), 2567–2590. https://doi.org/10.5194/gmd-10-2567-2017

Lawrence, D. M., Fisher, R. A., Koven, C. D., Oleson, K. W., Swenson, S. C., Bonan, G., et al. (2019). The Community Land Model version 5: Description of new features, benchmarking, and impact of forcing uncertainty. *Journal of Advances in Modeling Earth Systems*, *11*, 4245–4287. https://doi.org/10.1029/2018MS001583

Luo, Y., Zhang, X., Wang, X., & Lu, F. (2014). Biomass and its allocation of Chinese forest ecosystems. *Ecology*, *95*(7), 2026–2026. https://doi.org/10.1890/13-2089.1

Luo, Y. Q., Randerson, J. T., Abramowitz, G., Bacour, C., Blyth, E., Carvalhais, N., et al. (2012). A framework for benchmarking land models. *Biogeosciences*, *9*(10), 3857–3874. https://doi.org/10.5194/bg-9-3857-2012

Malhi, Y., Doughty, C., & Galbraith, D. (2011). The allocation of ecosystem net primary productivity in tropical forests. *Philosophical Transactions of the Royal Society B: Biological Sciences*, *366*(1582), 3225–3245. https://doi.org/10.1098/rstb.2011.0062

McDowell, N. G., Allen, C. D., Anderson-Teixeira, K., Aukema, B. H., Bond-Lamberty, B., Chini, L., et al. (2020). Pervasive shifts in forest dynamics in a changing world. *Science*, *368*(6494), eaaz9463. https://doi.org/10.1126/science.aaz9463

Michaletz, S. T., Cheng, D., Kerkhoff, A. J., & Enquist, B. J. (2014). Convergence of terrestrial plant production across global climate gradients. *Nature*, *512*(7512), 39–43. https://doi.org/10.1038/nature13470

Negrón-Juárez, R. I., Koven, C. D., Riley, W. J., Knox, R. G., & Chambers, J. Q. (2015). Observed allocations of productivity and biomass, and turnover times in tropical forests are not accurately represented in CMIP5 Earth system models. *Environmental Research Letters*, *10*(6), 064107. https://doi.org/10.1088/1748-9326/10/6/064017

Niklas, K. J. (1995). Size-dependent allometry of tree height, diameter and trunk-taper. *Annals of Botany*, *75*, 217–227. https://doi.org/10.1006/anbo.1995.1015

Niklas, K. J. (2004). Plant allometry: Is there a grand unifying theory? *Biological Reviews*, *79*(4), 871–889. https://doi.org/10.1017/s1464793104006499

Oleson, K. W., Lawrence, D. M., Gordon, B., Flanner, M. G., Kluzek, E., Peter, J., et al. (2010). Technical description of version 4.0 of the Community Land Model (CLM). NCAR Technical Note NCAR/TN-478+STR, 257pp. https://doi.org/10.5065/D6FB50WZ

Peichl, M., & Arain, M. A. (2006). Above- and belowground ecosystem biomass and carbon pools in an age-sequence of temperate pine plantation forests. *Agricultural and Forest Meteorology*, *140*(1–4), 51–63. https://doi.org/10.1016/j.agrformet.2006.08.004

Pelt, R. V., & Sillett, S. C. (2008). Crown development of coastal *pseudotsuga menziesii*, including a conceptual model for tall conifers. *Ecological Monographs*, *78*(2), 283–311. https://doi.org/10.1890/07-0158.1

Phillips, N. G., Buckley, T. N., & Tissue, D. T. (2008). Capacity of old trees to respond to environmental change. *Journal of Integrative Plant Biology*, *50*(11), 1355–1364. https://doi.org/10.1111/j.1744-7909.2008.00746.x

Poorter, H., Jagodzinski, A. M., Ruiz-Peinado, R., Kuyah, S., Luo, Y., Oleksyn, J., et al. (2015). How does biomass distribution change with size and differ among species? An analysis for 1200 plant species from five continents. *New Phytologist*, *208*(3), 736–749. https://doi.org/10.1111/nph.13571

Pugh, T. A. M., Lindeskog, M., Smith, B., Poulter, B., Arneth, A., Haverd, V., & Calle, L. (2019). Role of forest regrowth in global carbon sink dynamics. *Proceedings of the National Academy of Sciences*, *116*(10), 4382–4387. https://doi.org/10.1073/pnas.1810512116

Reichstein, M., Camps-Valls, G., Stevens, B., Jung, M., Denzler, J., & Carvalhais, N. (2019). Deep learning and process understanding for data-driven Earth system science. *Nature*, *566*(7743), 195–204. https://doi.org/10.1038/s41586-019-0912-1

Reick, C. H., Raddatz, T., Brovkin, V., & Gayler, V. (2013). Representation of natural and anthropogenic land cover change in MPI-ESM. *Journal of Advances in Modeling Earth Systems*, *5*, 459–482. https://doi.org/10.1002/jame.20022

Sato, H., Itoh, A., & Kohyama, T. (2007). SEIB–DGVM: A new Dynamic Global Vegetation Model using a spatially explicit individual-based approach. *Ecological Modelling*, *200*(3–4), 279–307. https://doi.org/10.1016/j.ecolmodel.2006.09.006

Schepaschenko, D., Shvidenko, A., Usoltsev, V., Lakyda, P., Luo, Y., Vasylyshyn, R., et al. (2017). A dataset of forest biomass structure for Eurasia. *Scientific Data*, *4*(1), 1–11. https://doi.org/10.1038/sdata.2017.70

Séférian, R., Nabat, P., Michou, M., Saint-Martin, D., Voldoire, A., Colin, J., et al. (2019). Evaluation of CNRM Earth system model, CNRM-ESM 2-1: Role of Earth system processes in present-day and future climate. *Journal of Advances in Modeling Earth Systems*, *11*, 4182–4227. https://doi.org/10.1029/2019MS001791

Seidl, R., Schelhaas, M. J., Rammer, W., & Verkerk, P. J. (2014). Increasing forest disturbances in Europe and their impact on carbon storage. *Nature Climate Change*, *4*(9), 806–810. https://doi.org/10.1038/nclimate2318

Seland, Ø., Bentsen, M., Seland Graff, L., Olivié, D., Toniazzo, T., Gjermundsen, A., et al. (2020). The Norwegian Earth system model, NorESM2—Evaluation of the CMIP6 DECK and historical simulations. *Geoscientific Model Development Discussions*, 1–68. https://doi.org/10.5194/gmd-2019-378

Sheil, D., Eastaugh, C. S., Vlam, M., Zuidema, P. A., Groenendijk, P., Sleen, P., et al. (2017). Does biomass growth increase in the largest trees? Flaws, fallacies and alternative analyses. *Functional Ecology*, *31*(3), 568–581. https://doi.org/10.1111/1365-2435.12775

Shevliakova, E., Pacala, S. W., Malyshev, S., Hurtt, G. C., Milly, P. C. D., Caspersen, J. P., et al. (2009). Carbon cycling under 300 years of land use change: Importance of the secondary vegetation sink. *Global Biogeochemical Cycles*, *23*, GB2022. https://doi.org/10.1029/2007GB003176

Sillett, S. C., Van Pelt, R., Koch, G. W., Ambrose, A. R., Carroll, A. L., Antoine, M. E., & Mifsud, B. M. (2010). Increasing wood production through old age in tall trees. *Forest Ecology and Management*, *259*(5), 976–994. https://doi.org/10.1016/j.foreco.2009.12.003

Sitch, S., Smith, B., Prentice, I. C., Arneth, A., Bondeau, A., Cramer, W., et al. (2003). Evaluation of ecosystem dynamics, plant geography and terrestrial carbon cycling in the LPJ dynamic global vegetation model. *Global Change Biology*, *9*(2), 161–185. https://doi.org/10.1046/j.1365-2486.2003.00569.x

Smith, B. (2001). LPJ-GUESS—An ecosystem modelling framework. *Department of Physical Geography and Ecosystems Analysis. INES. Sölvegatan*, *12*, 22362.

Song, X., Hoffman, F. M., Iversen, C. M., Yin, Y., Kumar, J., Ma, C., & Xu, X. (2017). Significant inconsistency of vegetation carbon density in CMIP5 Earth system models against observational data. *Journal of Geophysical Research: Biogeosciences*, *122*, 2282–2297. https://doi.org/10.1002/2017JG003914

Stephenson, N. L., Das, A. J., Condit, R., Russo, S. E., Baker, P. J., Beckman, N. G., et al. (2014). Rate of tree carbon accumulation increases continuously with tree size. *Nature*, *507*(7490), 90–93. https://doi.org/10.1038/nature12914

Swart, N. C., Cole, J. N. S., Kharin, V. V., Lazare, M., Scinocca, J. F., Gillett, N. P., et al. (2019). The Canadian Earth system model version 5 (CanESM5.0.3). *Geoscientific Model Development*, *12*(11), 4823–4873. https://doi.org/10.5194/gmd-12-4823-2019

Tjiputra, J., Roelandt, C., Bentsen, M., Lawrence, D., Lorentzen, T., Schwinger, J., et al. (2013). Evaluation of the carbon cycle components in the Norwegian Earth system model (NorESM). *Geoscientific Model Development*, *6*(2), 301–325. https://doi.org/10.5194/gmd-6-301-2013

Watanabe, S., Hajima, T., Sudo, K., Nagashima, T., Takemura, T., Okajima, H., et al. (2011). MIROC-ESM 2010: Model description and basic results of CMIP5-20c3m experiments. *Geoscientific Model Development*, *4*(4), 845–872. https://doi.org/10.5194/gmd-4-845-2011

West, G. B., Brown, J. H., & Enquist, B. J. (1999). A general model for the structure and allometry of plant vascular systems. *Nature*, *400*(6745), 664–667.

Williams, C. A., Collatz, G. J., Masek, J., & Goward, S. N. (2012). Carbon consequences of forest disturbance and recovery across the conterminous United States. *Global Biogeochemical Cycles*, *26*, GB1005. https://doi.org/10.1029/2010GB003947

Wu, D., Piao, S., Liu, Y., Ciais, P., & Yao, Y. (2018). Evaluation of CMIP5 Earth system models for the spatial patterns of biomass and soil carbon turnover times and their linkage with climate. *Journal of Climate*, *31*(15), 5947–5960. https://doi.org/10.1175/jcli-d-17-0380.1

Xia, J., McGuire, A. D., Lawrence, D., Burke, E., Chen, G., Chen, X., et al. (2017). Terrestrial ecosystem model performance in simulating productivity and its vulnerability to climate change in the northern permafrost region. *Journal of Geophysical Research: Biogeosciences*, *122*, 430–446. https://doi.org/10.1002/2016JG003384

Xia, J., Wang, J., & Niu, S. (2020). Research challenges and opportunities for using big data in global change biology. *Global Change Biology*, *26*(11), 6040–6061. https://doi.org/10.1111/gcb.15317

Xia, J., Yuan, W., Lienert, S., Joos, F., Ciais, P., Viovy, N., et al. (2019). Global patterns in net primary production allocation regulated by environmental conditions and forest stand age: A model-data comparison. *Journal of Geophysical Research: Biogeosciences*, *124*, 2039–2059. https://doi.org/10.1029/2018JG004777

Yan, Y., Luo, Y., Zhou, X., & Chen, J. (2014). Sources of variation in simulated ecosystem carbon storage capacity from the 5th Climate Model Intercomparison Project (CMIP5). *Tellus B: Chemical and Physical Meteorology*, *66*(1), 22568. https://doi.org/10.3402/tellusb.v66.22568

Yang, X., Richardson, T. K., & Jain, A. K. (2010). Contributions of secondary forest and nitrogen dynamics to terrestrial carbon uptake. *Biogeosciences*, *7*(10), 3041–3050. https://doi.org/10.5194/bg-7-3041-2010

Yue, C., Ciais, P., Luyssaert, S., Li, W., McGrath, M. J., Chang, J., & Peng, S. (2018). Representing anthropogenic gross land use change, wood harvest, and forest age dynamics in a global vegetation model ORCHIDEE-MICT v8.4.2. *Geoscientific Model Development*, *11*(1), 409–428. https://doi.org/10.5194/gmd-11-409-2018

Yukimoto, S. (2011). Meteorological Research Institute-Earth system model version 1 (MRI-ESM 1)—MODEL description. *Technical Reports of the Meteorological Research Institute*. https://doi.org/10.11483/mritechrepo.64

Yukimoto, S., Kawai, H., Koshiro, T., Oshima, N., Yoshida, K., Urakawa, S., et al. (2019). The Meteorological Research Institute Earth system model version 2.0, MRI-ESM 2.0: Description and basic evaluation of the physical component. *Journal of the Meteorological Society of Japan. Ser. II*, *97*(5), 931–965. https://doi.org/10.2151/jmsj.2019-051

Zaehle, S., Sitch, S., Prentice, I. C., Liski, J., Cramer, W., Erhard, M., et al. (2006). The importance of age-related decline in forest NPP for modeling regional carbon balances. *Ecological Applications*, *16*(4), 1555–1574. https://doi.org/10.1890/1051-0761(2006)016[1555:tioadi]2.0.co;2

Zhang, Y., Yao, Y., Wang, X., Liu, Y., & Piao, S. (2017). Mapping spatial distribution of forest age in China. *Earth and Space Science*, *4*, 108–116. https://doi.org/10.1002/2016EA000177

Zhu, C., Cui, E., & Xia, J. (2020). Both day and night warming reduce tree growth in extremely dry soils. *Environmental Research Letters*, *15*(9), 094074. https://doi.org/10.1088/1748-9326/aba65e